

NATL INST. OF STAND & TECH



A11107 214309

NIST  
PUBLICATIONS

**NIST**

REFERENCE

National Institute of  
Standards and Technology  
U.S. Department of Commerce

*NIST Technical Note 1556*

**Multimode Fiber Launch Study: Estimating  
the Impact on Measurements of Propagation  
Delay**

**Tasshi Dennis**

QC  
100  
.U5753  
#1556  
2010



**Multimode Fiber Launch Study: Estimating the Impact on Measurements of Propagation Delay**

---

Tasshi Dennis  
*Electromagnetics and Electrical Engineering Laboratory  
National Institute of Standards and Technology  
Boulder, CO 80305-3328*

August 2010



**U.S. Department of Commerce**  
*Gary Locke, Secretary*

**National Institute of Standards and Technology**  
*Patrick Gallagher, Director*

---

National Institute of Standards  
and Technology  
Technical Note 1556  
Natl. Inst. Stand. Technol.  
Tech. Note 1556  
**14 pages** (August 2010)  
CODEN: NTNOEF

U.S. Government Printing Office  
Washington: 2010

For Sale by the  
Superintendent of Documents  
U.S. Government Printing Office  
Stop SSOP, Washington, DC 20402-0001  
Phone: (202) 512-1800  
Fax: (202) 512-2250  
Internet: [bookstore.gpo.gov](http://bookstore.gpo.gov)

# Multimode Fiber Launch Study: Estimating the Impact on Measurements of Propagation Delay

Tasshi Dennis

National Institute of Standards and Technology  
Boulder, Colorado 80305

## Executive Summary

The purpose of this study was to evaluate measurement uncertainties introduced into propagation time delay calibrations of multimode fiber reference spools, as well as their use as transfer standards. While the principles described are generally applicable, the results could be different for other types of available multimode fiber and should be evaluated on an individual basis. The study was conducted by use of a high-accuracy NIST technique for measuring delay, and again the results obtained could be different, and with higher uncertainty, for more conventional measurement methods. To that end, we also considered some limiting cases that could be encountered with conventional measurement equipment, and examined the performance of one commercial instrument. The results of this study are presented along with suggested guidance and areas for future study.

## Introduction

The measured time delay of a multimode (MM) optical fiber can depend on the spatial optical modes launched into the fiber to measure the delay. This dependence on the launch conditions is caused by modal dispersion, which is a specific characteristic of a MM fiber design [1, 2]. Illustrated in Fig. 1(a) is a simplistic ray view of why different modes, represented by different launch angles, have different path lengths and therefore different time delays in what is known as a step-index fiber. The square-top index profile is shown to the right. Typically, a steeper launch angle results in a longer delay because the light ray experiences more internal reflections at the core-cladding boundary. Therefore, an optical pulse launched into two different modes of a fiber may experience broadening in time or it may even separate into two distinct pulses [1, 2]. One way to counter this modal dispersion is to make the refractive index profile of the fiber higher at the center of the core than it is at the boundary with the cladding [1, 2]. A common index profile is parabolic in shape, as shown in Fig. 1(b), and is described as a graded-index fiber. The profile equalizes the path lengths despite different launch angles. In the latest, high-bandwidth multimode optical networks, the engineering assumption is that the graded-index profile can be tailored so precisely to the application that modal dispersion is negligible. However, the effect of dispersion may not be negligible relative to the low uncertainties required for the delay calibration of multimode fiber reference spools. Also, this assumption is generally

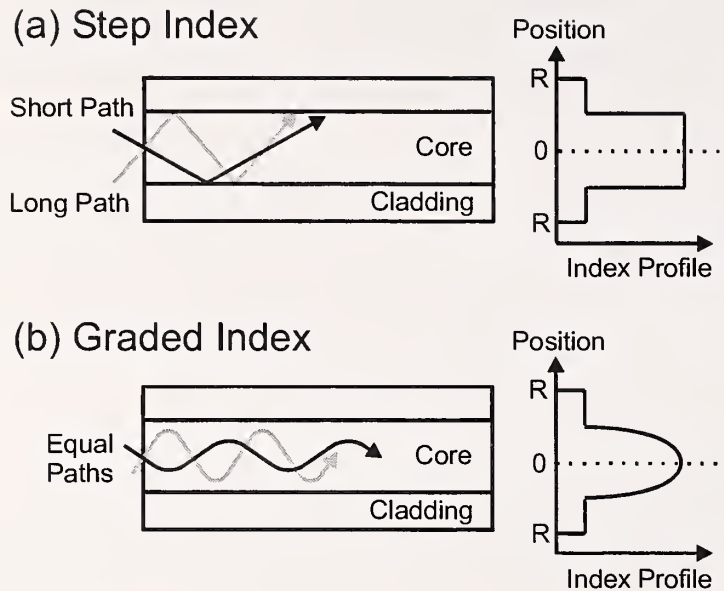


Fig. 1: Multimode ray propagation and index profiles for (a) step-index and (b) graded-index fiber.

not true for legacy MM optical fiber, due to alternate design criteria and variations at the time of manufacture. Such legacy fiber was typically designed for a launch that filled as many modes as possible by use of a broadband source and not for high-bandwidth applications employing the launch of at most a few modes with a narrow linewidth laser. When used in high-bandwidth communications links, legacy fiber can introduce significant optical delay line artifacts. It is important to characterize the dependence of the delay on the mode launch conditions for the given type of fiber. Such a study requires that one have a method for both controlling and measuring the launch conditions, and measuring the fiber delay.

### Conventional Fiber Delay Measurement Instrumentation

The most common field instrument for measuring the time delay of an optical fiber is the optical time-domain reflectometer (OTDR). In an OTDR, short optical pulses are launched into the fiber under test and the back reflection of the pulses is monitored by the instrument as a function of time. The return light is generated throughout the fiber span both continuously from Rayleigh scattering and abruptly from Fresnel reflections occurring at fiber terminations, splices, faults, and optical components. The time delay is measured as half the round-trip period for the pulse to reflect and return from the far end of the fiber being measured. The physical length of the fiber can be calculated from the time delay by use of the group refractive index, but only to the level of uncertainty that the value of the index is known for that fiber.

For the measurement of multimode fiber, the optical pulse source inside the OTDR can be a laser or a light-emitting diode (LED). Legacy OTDRs have typically used lasers to achieve high output power and short pulses, but typically do not consider the modal launch conditions.



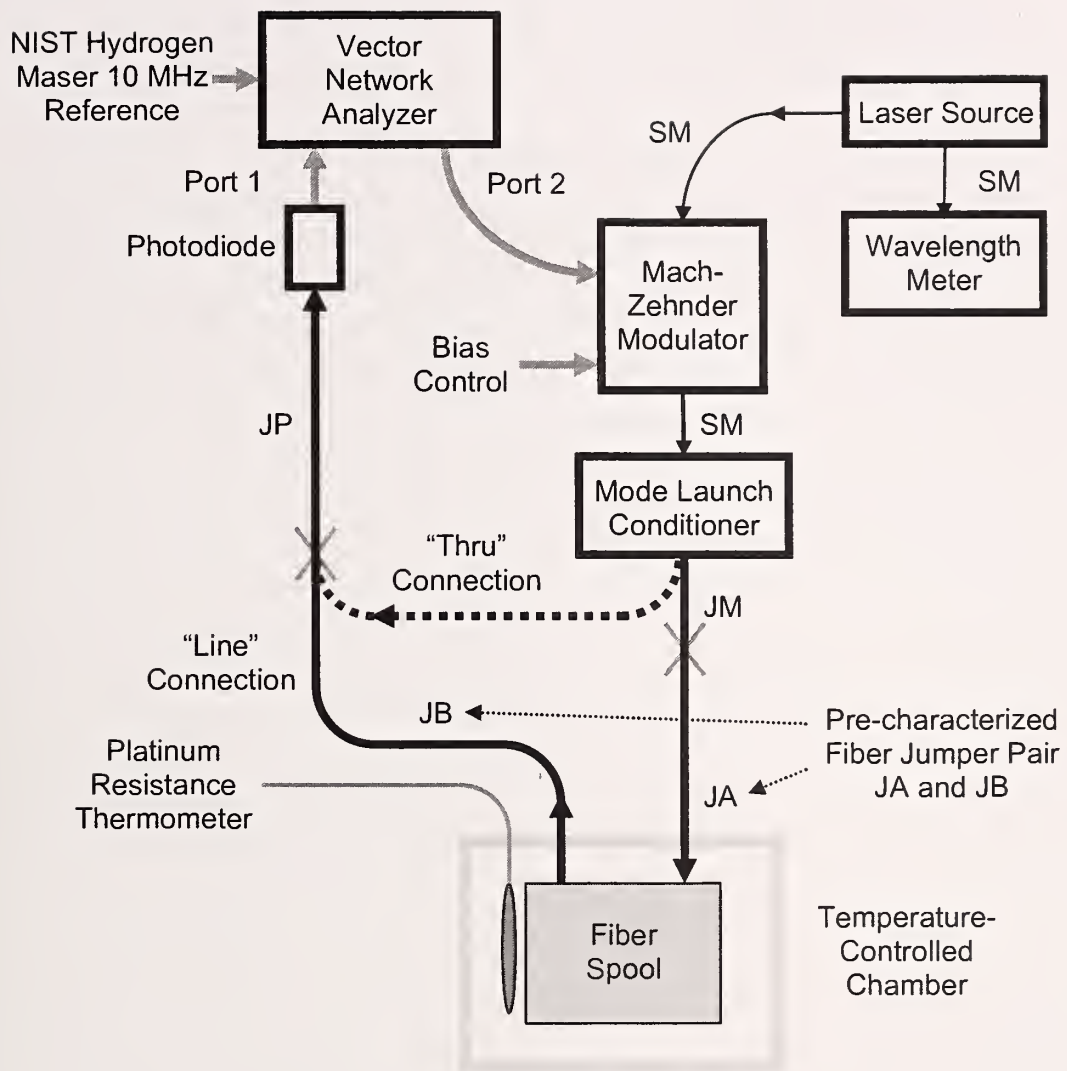


Fig. 2: Schematic of fiber group delay measurement apparatus. Thick black lines represent multi-mode optical paths; thin black lines represent single-mode (SM) optical paths; gray lines represent electrical paths. The gray "X" symbols represent FC/PC connections that are changed manually during the calibration process. The fiber cable JP connected to the photodiode can be connected directly to the Mach-Zehnder modulator jumper JM for a "thru" connection, or to jumper JB from the fiber spool for the "line" connection. The temperature of the spool is stabilized in one of three ovens. Each oven has a corresponding jumper pair (denoted JA and JB) used to connect the fiber spool to the measurement system.

Modern OTDRs intended for Ethernet testing typically make use of high-power LEDs, with the intent of controlling the modal launch conditions relative to industry standards. As we will show, the type of source utilized in an OTDR and the particular launch conditions it offers will have an influence on the delay that is observed for a particular multimode optical fiber.

### NIST Fiber Delay Measurement Technique

We measured the group delay of multimode optical fibers with a frequency-domain “phase-shift” technique similar to those described in references [3-5]. A schematic diagram of the apparatus used is shown in Fig. 2. The laser source generated a stable continuous emission with wavelength at 850 nm. Output port 2 of a vector network analyzer (VNA) drove the Mach-Zehnder modulator with sine waves, modulating the laser source. The sine wave frequency was stepped from 30 kHz to 1 GHz in increments of about 1.25 MHz. The optical signal traveled to the photodiode via the “thru” connection (via JM and JP in Fig. 2, excluding the fiber spool) or via the “line” connection (via the pre-characterized jumper pair JA and JB connected to JM and JP, respectively, and the fiber spool being calibrated). The photodiode converted the modulation on the optical signal back to an electrical signal, and the VNA calculated the complex ratio of the received electrical signal to the generated electrical signal. Measurements of this ratio were acquired for each frequency  $f_j$  ( $j = 1, \dots, 801$ ) via an external computer for later processing. The connection to the photodiode was changed manually from the “thru” connection to the “line” connection, with measurements collected from both configurations. The phase delay of the modulation envelope after traveling through the fiber spool and jumper pair was found, modulo  $2\pi$ , from the phase of the ratio of the “line” measurement to the “thru” measurement:

$$\frac{z_{\text{line}}}{z_{\text{thru}}} = \rho(f_j) e^{i\phi(f_j)}, \quad (1)$$

where  $z_{\text{line}}$  and  $z_{\text{thru}}$  are the complex ratios measured by the VNA for the “line” and “thru” connections, respectively. Both of these measurements included effects due to the frequency dependent mismatch and loss of the Mach-Zehnder modulator and the couplers in the VNA. Because these effects were constant for the two measurements, they canceled in Eq. (1), and what remained were contributions that were different in the two measurements. These included the loss and insertion delay of the spool and jumper pair that were to be calculated, as well as some small effects due to multi-path interference between the fiber connectors. These interference effects were kept to a minimum by use of physical contact connections of high return loss ( $> 30$  dB) throughout the system.

Equation (1) gives the phase  $\phi(f_j)$  of the modulation envelope modulo  $2\pi$  and the magnitude of the modulation envelope, which was not needed for these calculations. The actual phase delay  $\Phi(f_j)$  due to the fiber spool is related to the phase in Eq. (1) by

$$\Phi(f_j) = 2\pi m + \phi(f_j), \quad (2)$$



where  $m$  is an unknown integer and a function of the frequency  $f_j$ . The group delay  $\tau$  of the fiber is

$$\tau = \frac{\Phi(f_j)}{2\pi f_j}. \quad (3)$$

Because  $m$  is unknown, an iterative method was used to estimate  $\tau$  as follows:

1. Pick an initial guess  $\tau^*$  for  $\tau$ . For a 600 meter fiber, a reasonable guess would be  $\tau^* = Ln_g/c = 2964$  ns, where  $L$  is the length of the fiber,  $n_g = 1.481$  is the group index of the fiber [6], and  $c$  is the speed of light in vacuum.
2. Calculate the deviation of the measured phase from the estimated phase by use of the estimate in step 1:

$$\Delta\phi_j = \arg\left(\frac{z_{\text{line}}}{z_{\text{thru}}}\exp(i2\pi f_j \tau^*)\right). \quad (4)$$

3. At the lowest frequency, assume the error  $\Delta\tau_0 = 0$ . Then

$$\Delta\tau_j = \frac{1}{f_j}\left(\frac{\Delta\phi_j}{2\pi} + \text{integer}(\Delta\tau_{j-1}f_j)\right). \quad (5)$$

4. The  $j$ th estimate of the group delay is  $\tau_j = \tau^* - \Delta\tau_j$ . The algorithm typically converges as shown by the gray dots in Fig 3. Several visual and analytic cross checks are used to verify convergence to the correct value.
5. To average over ripples caused by multi-path interference and speckle, the average group delay  $\bar{\tau}$  over the frequencies between 250 MHz and 1000 MHz was calculated:

$$\bar{\tau} = \text{mean}(\tau_{250\text{MHz}}, \dots, \tau_{1000\text{MHz}}). \quad (6)$$

In Fig. 3,  $\bar{\tau}$  is shown as the dashed horizontal line.

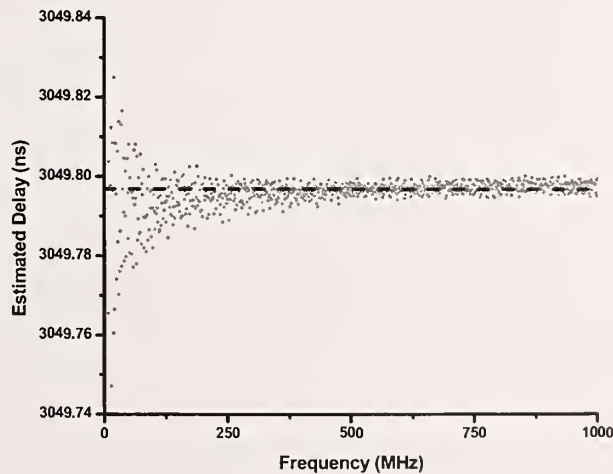


Fig. 3: Typical convergence of the estimated group delay with increasing frequency, from data analysis steps 3 and 4. The dashed line is the average group delay from step 5.

## Control of Modal Launch

The modal launch system we constructed is illustrated in Fig. 4. In our frequency-domain “phase-shift” method for measuring the fiber time delay, we minimized the impact due to chromatic dispersion by using a laser precisely tuned to 850.00 nm. This choice then required that we externally modulate the source with a Mach-Zehnder modulator, optimized for 850 nm. The output fiber of the modulator was single-mode (SM) at 850 nm (5/125  $\mu\text{m}$  core/cladding). This created the very challenging task of forming a multimode launch out of a monochromatic single-mode launch. We were able to do this through a series of processing steps that incurred a total optical loss of 10 to 13 dB. The first step was a radial over-filled launch [7] between the SM fiber and a graded-index MM fiber. This device was essentially a variable air-gap between the optical connectors of the two types of fiber, which allowed the spatial cone of the SM launch to spread out over the end face of the MM fiber. As the gap between the connectors was increased, the number of modes excited in the MM fiber increased. The end of the graded-index MM fiber was connected to a 3 meter step-index fiber that was looped and physically shaken to scramble the modal structure of the light in time. This speckle-averaging step reduced the spatial coherence of the light over observation periods that were much longer than the scrambling period. Static modal scrambling of the light was introduced by a serpentine wrapping of the step-index fiber. Finally, the light was launched back into a 10 meter graded-index fiber, which could be wrapped around a mandrel to strip off unwanted higher-order-modes. The 10 meter fiber also allowed for the natural spatial filtering of lossy cladding modes.

## Measurement of Modal Launch

We used a commercially available modal launch analyzer designed for the characterization of modal launch in high-bandwidth optical networks. The instrument precisely images the emitting end face of the multimode fiber onto a CCD camera. Image processing software is then used to calculate beam profile quantities from the image of the lit fiber, generally as a function of radial distance from the center of the fiber core. The mode power distribution, encircled flux, mode transfer function, and intensity profile are reported.

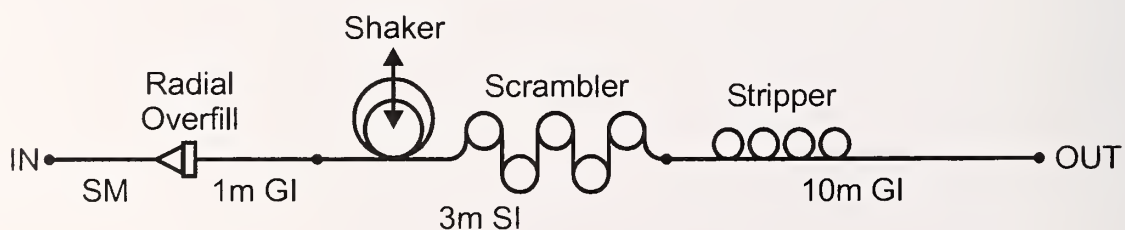


Fig. 4: Mode launch control system that converts a single mode (SM) input to a multimode output. The multimode fiber is either step-index (SI) or graded-index (GI) type.

## **Mode Launch Standards**

The mode launch analyzer was designed to comply with the measurement procedure for encircled flux specified by TIA/EIA standard FOTP-203: Launched Power Distribution Measurement Procedure for Graded-Index Multimode Fiber Transmitters [8]. The instrument also complies with the very recent standard specified in IEC 61280-4-1 for Fibre-Optic Communications Subsystem Test Procedures – Part 4-1: Installed Cable Plant – Multimode Attenuation Measurement [9]. In the IEC document, the encircled flux plays a critical role in achieving higher-accuracy attenuation measurements in 10G Ethernet networks. In that application, the fiber is assumed to have a perfect graded-index profile, resulting in no modal dispersion. However, the mechanical tolerance of connectors in these networks causes small misalignments of the fiber cores, which in turn create offset launch conditions that increase the uncertainty of optical loss measurements using optical time-domain reflectometers (OTDR's). Modeling has shown that measurement uncertainty can be reduced to an acceptable level by precisely specifying the encircled flux of test light launched by the OTDR. The IEC 61280-4-1 specification for encircled flux is a range given by a radial template; however it is very restrictive: at 20  $\mu\text{m}$  radius the tolerance is 1.90 % and at 22  $\mu\text{m}$  radius it is only 1.22 %.

While the IEC standard was developed with fiber loss measurements in mind, it does provide a convenient and fairly precise definition of a modal launch condition that will be found in future OTDR systems. As we have discussed, the modal launch condition can significantly influence the measurement of time delay, particularly in legacy fibers. Conforming to the restrictive launch condition specified by the IEC standard allows a level of control over the measured variation in time delay. However, because the standard specifies a template with upper and lower bounds, it is possible that various conforming launch conditions could still result in measurable variations in time delay. During a particular delay calibration, only a small subset of the infinite number of possible mode launch conditions passing the IEC encircled-flux criteria are generated. A secondary (user) laboratory may generate a different subset of passing IEC conditions, perhaps with little commonality to the launches used during the calibration. For this reason, we studied the impact of encircled flux mode launch conditions on the measured time delay, and used the results to estimate an uncertainty for our calibration system.

## **NIST Mode Launch Study**

To test the dependence of delay on modal launch, we generated different encircled-flux launch conditions, all of which conformed to the IEC 61280-4-1 specification. The bounds of the IEC encircled flux template for 50/125  $\mu\text{m}$  core/cladding fiber at 850 nm are shown by the black vertical lines in Fig. 5. We varied as many of the settings of our modal launch control system as possible to try to sample as much of the template range. We paid particular attention to the encircled-flux bounds at large radii (20  $\mu\text{m}$  and 22  $\mu\text{m}$ ), which are the most difficult criteria to meet in practice. These bounds are tight because the impact on measured attenuation accuracy is greatest: light propagating at large radii is most affected by connector misalignment and cladding loss.



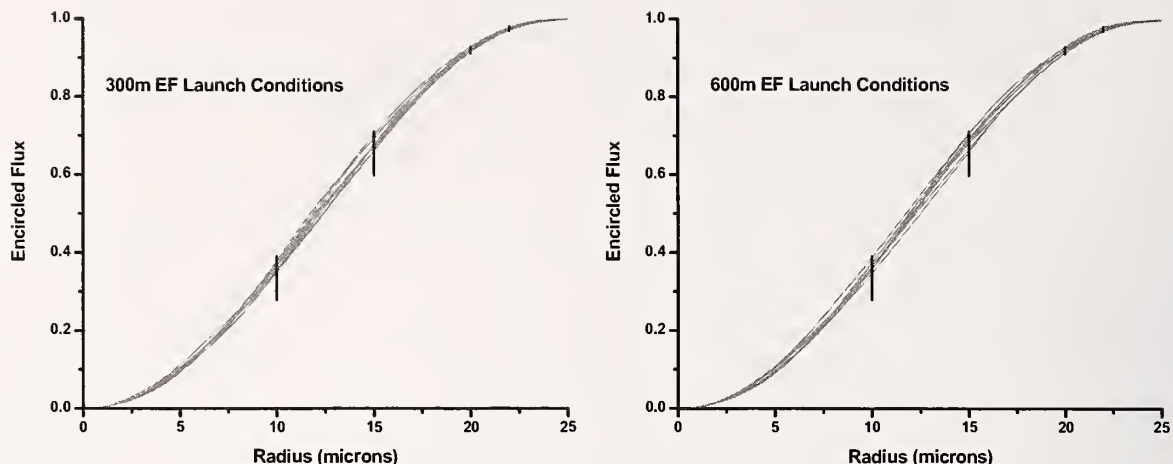


Fig. 5: IEC encircled-flux template specifications (four black lines in each plot) and the measured launch conditions generated for this study (gray curves).

We assumed that there is predominately a one-to-one mapping between encircled flux and measured delay, although it does seem likely that two different launch conditions could result in the same measured delay. We attempted to sample all of the range in delay variation by uniformly covering the encircled-flux bounds at large radii. Figure 5 shows the encircled-flux curves for different launch conditions that we created for measuring the delay of a 300 m and a 600 m length of Corning InfiniCor 50  $\mu\text{m}$  fiber [6]. In creating at least ten different conditions for each length of fiber, we often pushed our modal launch control system to the limits of its operating range. Some of the measured delay variation could have been caused by low launch powers; some conditions required a lot of radial over-filled launch and mandrel wrapping, both of which are lossy. Figure 6 shows histograms of the measured delays for both lengths of fiber, normalized to the nearest integer delay in nanoseconds. The histograms are coarse because of the finite number of measurements. However, despite differences in appearance, the standard deviations of the two sets of measurements are nearly equal.

Standard deviation of 10 measurements of 300 meter length: **0.00271 ns**

Standard deviation of 11 measurements of 600 meter length: **0.00263 ns**

The delay variation does not appear to depend on fiber length, which is consistent with the notion that the launch dependence is governed by propagation within the first few tens of meters. The time delay of a 300 m fiber is about 1500 ns, so the deviation we measured was on the order of 5 parts in  $10^5$ . We took the standard deviation as an uncertainty estimate for the measurement of delay caused by the mode launch conditions. In our method for calibration of time delay in multimode fibers, the uncertainty due to mode launch appeared twice: from measuring the fiber itself, and a separate measurement of the connecting jumper cables JA and JB. We combined

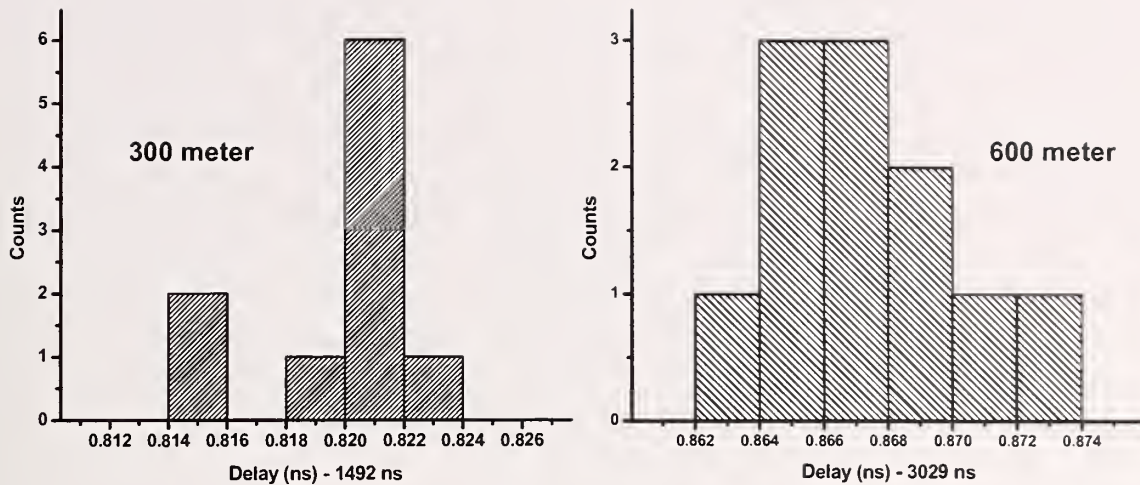


Fig. 6: Histograms of the measured time delay for varying modal launch conditions into 300 and 600 meter fibers. The horizontal axes have been normalized to the nearest integer delay in nanoseconds.

the two uncertainty contributions in quadrature [10], namely  $\sqrt{2} \times 0.00271$  ns, giving a total mode launch uncertainty of 0.0038 ns. The only other uncertainty contribution in our delay measurement method that is comparable to the total mode launch is the uncertainty due to the measurement of phase (0.0044 ns). Therefore, when constrained to the IEC launch specification, the uncertainty due to mode launch for this type of multimode fiber is significant but not the largest source of uncertainty.

We note that the results obtained here for variation in delay with launch conditions are specific to the fiber we measured. Substantially different results might have been obtained for other multimode fibers, including such variations as the manufacturer, core size, operating wavelength, and vintage.

### Some Limiting Cases

It is informative to consider some limiting cases for both encircled flux and variations in delay, in order to get a better sense for the magnitude of the effects in other situations. Outside of the encircled flux template are two distinct limiting cases: under-filled launch (UFL) and over-filled launch (OFL). While not strictly defined in terms of encircled flux, it is fairly easy to generate launch conditions that clearly fall within or near these two categories. In an OFL all or most of the modes of a multimode fiber are excited equally. This launch condition is typical of LED sources, which have a wide angular divergence, broad spectral bandwidth, and short temporal coherence. In a UFL only a few modes, perhaps just one, are excited. A UFL is easily generated from a narrow-band laser having a collimated beam with a narrow angular divergence and a long temporal coherence.



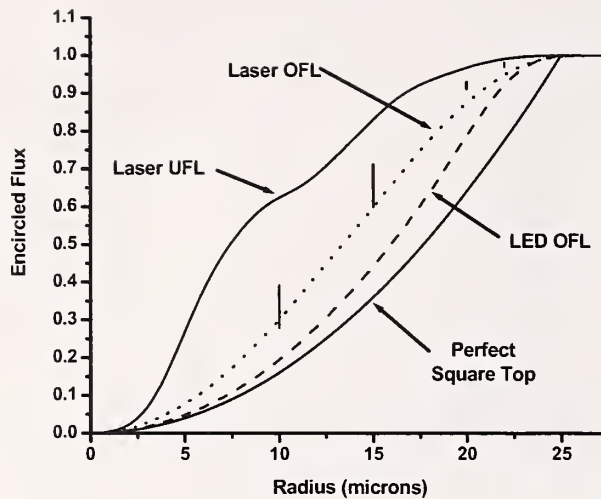


Fig. 7: The encircled-flux curves for some limiting mode launch conditions. The vertical bars indicate the IEC template bounds, as before. The “perfect square-top” profile is a calculated curve.

Figure 7 shows some limiting encircled-flux curves we generated for comparison to the IEC template (vertical bars). We created an OFL from an LED that had a singlemode fiber pigtail by using a combination of radial over-filled launch, speckle averaging, and a serpentine mode scrambler. The final output launch was delivered to the mode analyzer by use of a step index fiber, which gave an approximate square-top intensity profile. The encircled-flux curve for this LED OFL is well below the bounds of the IEC template. Shown for comparison is the calculated encircled flux for the limiting case of an ideal square-top intensity profile. The LED OFL launch lacked sufficient optical power to allow a fiber delay measurement under these conditions.

To have an OFL condition with sufficient light available for a delay measurement, we used a narrow-band laser source with our mode launch conditioner. An excessive degree of radial over-filled launch was required in order to generate the encircled-flux curve labeled “Laser OFL,” which is notable for the large deviation from the IEC template at 20  $\mu\text{m}$  and 22  $\mu\text{m}$  radii. This result represents our best effort at generating an OFL from a highly coherent source. Using this launch, we measured about a 12 ps difference in delay for a 600 m fiber compared to a launch that conforms to the IEC template. While this delay variation is significant, it represents a limiting case obtained from extreme conditions relative to how fiber delay is calibrated at NIST, and may be more indicative of older OTDRs with modulated LEDs and designed for legacy networks that employ LED sources.

As a final point of reference, we generated a UFL condition by using a narrowband laser launched from a singlemode fiber (5/125  $\mu\text{m}$  core/cladding). As shown in Fig. 7, the encircled flux curve is well above the IEC template bounds at all radii. While we made no rigorous delay measurements, we have observed that the delay in a 600 m fiber can vary by tens of picoseconds

compared to a qualified IEC launch. This launch condition is probably representative of legacy OTDRs based on lasers that pre-date multimode Ethernet testing with encircled-flux criteria.

### Conventional OTDR: A Specific Example

We characterized the mode launch conditions of a legacy OTDR of an early 1990's vintage [11], suitable for making conventional delay measurements using a source module designed for multimode fiber at 850 nm. The internal launch fiber of the OTDR had a 62.5  $\mu\text{m}$  core, so we attached additional launch fibers with 50  $\mu\text{m}$  cores and up to 11 m in length to condition the launch to match the fibers being measured for delay [6]. The launch conditions generated by the OTDR and measured by the mode analyzer are presented in Fig. 8, along with the IEC template bounds. The condition labeled "(a)" was generated from the OTDR with a 1 m launch fiber of 50  $\mu\text{m}$  core connected to the mode analyzer. This launch state was in the over-filled domain, having clearly missed the template at the 20  $\mu\text{m}$  and 22  $\mu\text{m}$  lower bounds. However, a single mandrel wrap (1" diameter) was sufficient to tune the launch to within the encircled-flux template. The three launch conditions labeled as "(b)" were generated from an 11 meter launch fiber and had OTDR pulse durations of 1 ns, 20 ns, and 100 ns. In each case, a single mandrel wrap was necessary to obtain a launch within the template bounds, as shown. The encircled flux appears to be largely independent of the pulse duration. Finally, the launch condition labeled "(c)" was generated with an 11 meter launch cord with six mandrel wraps, and clearly represents an under-filled launch by missing the upper template bounds at both 20  $\mu\text{m}$  and 22  $\mu\text{m}$ .

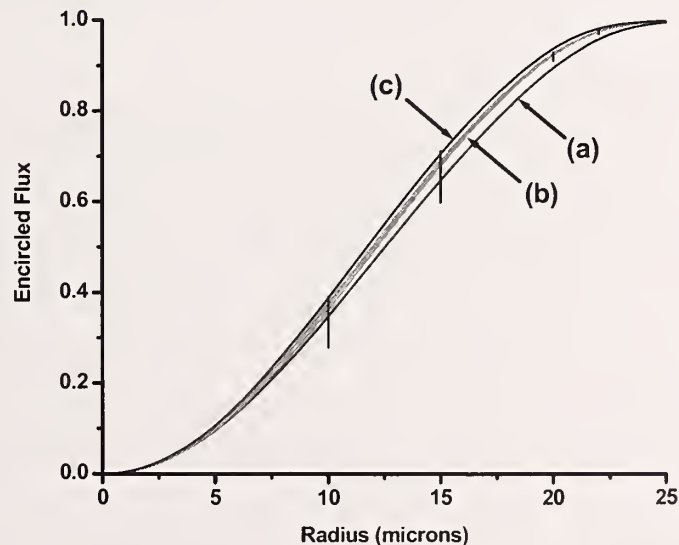


Fig. 8: Measured encircled-flux launch conditions of a conventional OTDR are presented. Launch (a) is from a 1 meter launch fiber attached to the OTDR. The three launches indicated by (b) are for pulses with 1 ns, 20 ns, and 100 ns duration and an 11 meter launch fiber with one mandrel wrap. Launch (c) includes 6 mandrel wraps and is above the template bounds.

The optical spectrum of the OTDR source module was measured with a grating-based optical spectrum analyzer. For pulse durations of 1 ns, 20 ns, and 100 ns the source spectrum had a full-width half-maximum bandwidth of about 3 nm, with an approximate Gaussian profile. This moderately broad bandwidth is more indicative of a multi-mode laser or superluminescent diode (SLED) rather than a highly-coherent DFB or highly-incoherent traditional LED. The spatial profile measured on the mode analyzer showed no strong signs of speckle noise, and as a result the need for speckle averaging did not appear critical.

We attempted to quantify the impact on delay as measured by the OTDR with two widely different launch conditions: an over-filled launch with no mandrel wraps, and an under-filled launch with 10 mandrel wraps. In its highest resolution mode using a 1 ns pulse, the OTDR provides a display resolution of 0.01 m or 1 cm. This corresponds to a temporal display resolution of only about 50 ps and is indicated by a reflection peak defined by multiple display points. As a result, we were unable to observe a difference in delay for the two launch conditions generated by this particular OTDR when measuring a 600 m fiber.

Nevertheless, the results are encouraging, because they indicate that this particular legacy OTDR is easily capable of generating qualified encircled-flux launch conditions, and in addition does not appear to require speckle averaging. This situation is a direct consequence of the source module utilized in this particular model of OTDR and is not representative of OTDRs in general, both new and old. That the impact of modal launch could not be observed here is both a result of the resolution offered by this particular OTDR and the type of fiber being measured. Measured in exactly this way, the launch conditions can be considered negligible.

### **Recommendations and Future Study**

The results of this study have estimated the impact of modal launch specific to the NIST measurement technique as well as a particular model of OTDR. The activities and results of this investigation provide some guidance and suggested areas for future study on the use of other conventional laser- and LED-OTDRs. At this time we offer the following recommendations:

1. Newly constructed reference spools should use modern fiber designed to minimize modal dispersion. Doing so will minimize the modal uncertainty contribution, although not necessarily eliminate it.
2. Reference spools containing legacy types of fiber should be characterized on a case-by-case basis for modal dispersion.
3. Use of an encircled-flux criterion to quantify and control the launch conditions of OTDR delay measurements will help minimize the modal uncertainty. The practicality of this approach depends largely on the nature of the OTDR light source.
4. The IEC encircled-flux standard is likely to be met with no modification and testing only by modern LED-OTDRs designed specifically for this standard.



5. It may be practical to convert the launch of some legacy OTDRs to the IEC standard, provided that a mode analyzer is used for quantification. Doing so would require further study to ensure compliance.
6. Laser-OTDRs will by nature generate an under-filled launch such that under a variety of conditions the modal launch uncertainty will dominate the total uncertainty budget.
7. For loss reasons, it is generally impractical to convert a laser-OTDR under-filled launch into an IEC encircled-flux launch.
8. The unit-to-unit variability in the launch conditions of existing laser-OTDRs should be studied and the variation in delay quantified.

### Acknowledgement

Funding for this study was provided by the US Air Force METCAL and US Army Aviation and Missile Command.

### References

- [1] J. Hecht, *Understanding Fiber Optics*, Prentice-Hall, 4th edition, chapter 4, 2002.
- [2] D. Cunningham, B. Lane, and W. Lane, *Gigabit Ethernet Networking*, Indianapolis: Macmillan Publishing Co. Inc, chapter 6, 1999.
- [3] S. E. Mechels, J. B. Schlager, and D. L. Franzen, "Accurate measurements of the zero-dispersion wavelength in optical fibers," *J. Res. Nat. Inst. Standards Technol.*, vol. 102, no. 3, 1997.
- [4] *Optical fibers, Part 1-22: Measurement methods and test procedures-Length measurement*, IEC International Standard 60793-1-22, IEC, 2001.
- [5] J. C. Bermudez and W. Schmid, "Characterization of an optical fiber spool to be used as reference standard for OTDRs distance scale calibration," *Proc. SPIE*, vol. 5776, pp. 102-108, SPIE, Bellingham, WA, 2005.
- [6] *Corning InfiniCor 50  $\mu$ m Optical Fibers – Product Information*, Corning Inc. product information sheet PI1457, available at [www.corning.com](http://www.corning.com), February 2010. NIST does not endorse product or trade names, which are stated here only to specify the experiment completely. Other products may be suitable yet produce different results.
- [7] D. Cunningham, B. Lane, and W. Lane, *Gigabit Ethernet Networking*, Indianapolis: Macmillan Publishing Co. Inc, p. 206, 1999.
- [8] *FOTP-203: Launched Power Distribution Measurement Procedure for Graded-Index Multimode Fiber Transmitters*, TIA/EIA Standard TIA/EIA-455-203, TIA/EIA, June 2001.

- [9] *Fibre-optic communication subsystem test procedures – Part 4-1: Installed cable plant – Multimode attenuation measurement*, IEC International Standard 61280-4-1, IEC, June 2009.
- [10] B. N. Taylor and C. E. Kuyatt, “Guidelines for evaluating and expressing the uncertainty of NIST measurement results,” *NIST Tech. Note 1297*, NIST, Boulder, CO, Sept. 1994.
- [11] Tektronix FiberMaster TFP2 with FM8500 multimode optical module. NIST does not endorse product or trade names, which are stated here only to specify the experiment completely. Other products may be suitable yet produce different results.



# *NIST Technical Publications*

## *Periodical*

---

**Journal of Research of the National Institute of Standards and Technology**—Reports NIST research and development in metrology and related fields of physical science, engineering, applied mathematics, statistics, biotechnology, and information technology. Papers cover a broad range of subjects, with major emphasis on measurement methodology and the basic technology underlying standardization. Also included from time to time are survey articles on topics closely related to the Institute's technical and scientific programs. Issued six times a year.

## *Nonperiodicals*

---

**Monographs**—Major contributions to the technical literature on various subjects related to the Institute's scientific and technical activities.

**Handbooks**—Recommended codes of engineering and industrial practice (including safety codes) developed in cooperation with interested industries, professional organizations, and regulatory bodies.

**Special Publications**—Include proceedings of conferences sponsored by NIST, NIST annual reports, and other special publications appropriate to this grouping such as wall charts, pocket cards, and bibliographies.

**National Standard Reference Data Series**—Provides quantitative data on the physical and chemical properties of materials, compiled from the world's literature and critically evaluated. Developed under a worldwide program coordinated by NIST under the authority of the National Standard Data Act (Public Law 90-396). NOTE: The Journal of Physical and Chemical Reference Data (JPCRD) is published bimonthly for NIST by the American Institute of Physics (AIP). Subscription orders and renewals are available from AIP, P.O. Box 503284, St. Louis, MO 63150-3284.

**Building Science Series**—Disseminates technical information developed at the Institute on building materials, components, systems, and whole structures. The series presents research results, test methods, and performance criteria related to the structural and environmental functions and the durability and safety characteristics of building elements and systems.

**Technical Notes**—Studies or reports which are complete in themselves but restrictive in their treatment of a subject. Analogous to monographs but not so comprehensive in scope or definitive in treatment of the subject area. Often serve as a vehicle for final reports of work performed at NIST under the sponsorship of other government agencies.

**Voluntary Product Standards**—Developed under procedures published by the Department of Commerce in Part 10, Title 15, of the Code of Federal Regulations. The standards establish nationally recognized requirements for products, and provide all concerned interests with a basis for common understanding of the characteristics of the products. NIST administers this program in support of the efforts of private-sector standardizing organizations.

*Order the following NIST publications—FIPS and NISTIRs—from the National Technical Information Service, Springfield, VA 22161.*

**Federal Information Processing Standards Publications (FIPS PUB)**—Publications in this series collectively constitute the Federal Information Processing Standards Register. The Register serves as the official source of information in the Federal Government regarding standards issued by NIST pursuant to the Federal Property and Administrative Services Act of 1949 as amended, Public Law 89-306 (79 Stat. 1127), and as implemented by Executive Order 11717 (38 FR 12315, dated May 11, 1973) and Part 6 of Title 15 CFR (Code of Federal Regulations).

**NIST Interagency or Internal Reports (NISTIR)**—The series includes interim or final reports on work performed by NIST for outside sponsors (both government and nongovernment). In general, initial distribution is handled by the sponsor; public distribution is handled by sales through the National Technical Information Service, Springfield, VA 22161, in hard copy, electronic media, or microfiche form. NISTIR's may also report results of NIST projects of transitory or limited interest, including those that will be published subsequently in more comprehensive form.

**U.S. Department of Commerce**  
National Bureau of Standards and Technology  
325 Broadway  
Boulder, CO 80305-3328

**Official Business**  
Penalty for Private Use \$300